Taylor & Francis
Taylor & Francis Group

Ginsenoside Rg3 attenuates pulmonary fibrosis by inhibiting endothelial to mesenchymal transition

Eunsik Yun[a], Byung Su Kwon[b], Jongmin Kim[a,c] and Aram Lee[a,c]

[a]Division of Biological Sciences, Sookmyung Women's University, Seoul, Korea; [b]Department of Obstetrics and Gynecology, Kyung Hee University Medical Center, Seoul, Korea; [c]Research Institute for Women's Health, Sookmyung Women's University, Seoul, Korea

ABSTRACT

Pulmonary fibrosis (PF) is a progressive and chronic lung disease characterized by excessive extracellular matrix (ECM) deposition and fibroblast proliferation. Endothelial-to-mesenchymal transition (EndMT) serves as a source of fibroblasts and contributes to PF progression. Ginsenoside Rg3 (Rg3), a steroidal saponin extracted from ginseng, is known to have pharmacological effects on vascular diseases. We have previously demonstrated that Rg3 inhibits EndMT and prevents endothelial dysfunction. Thus, we hypothesized that Rg3 may be a potential therapeutic agent for PF-targeting EndMT. EndMT occurs in the lung tissue of a bleomycin-induced PF mouse model, which was confirmed by co-staining of endothelial and mesenchymal markers in the pulmonary vasculature and changes in the expression of these markers. Rg3 administration decreased EndMT and suppressed PF development. We also examined the effect of Rg3 in an *in vitro* EndMT model induced by co-treatment with TGF-β2 and IL-1β. Rg3 treatment alleviated the characteristics of EndMT such as spindle-shaped morphological changes, EndMT marker expression changes, Dil-Ac-LDL uptake and migratory properties. In addition, we demonstrated the mechanism by which Rg3 inhibits EndMT by regulating the Smad2/3 signaling pathway. Collectively, Rg3 can be a potential therapeutic agent for PF using the EndMT inhibition strategy, furthermore, it can be considered Rg3 as a therapeutic candidate for various EndMT-associated vascular diseases.

Introduction

Idiopathic pulmonary fibrosis (IPF), the most common and aggressive form of interstitial lung disease, is a life-threatening disease because no effective treatment is available, even though efforts to demonstrate the precise mechanisms and develop drugs have been made over a few decades (Todd et al. 2012; Kai et al. 2017; Assayag et al. 2021). Unfortunately, it has been reported that the number of patients with IPF has increased over time (Liu et al. 2017). Pulmonary fibrosis (PF) is characterized by abnormal accumulation of the extracellular matrix (ECM), alveolar epithelial cell damage, vascular remodeling, and irreversible lung damage (Todd et al. 2012; Liu et al. 2017; Roh et al. 2021). Previous studies have focused on inflammation as an important cause of pathogenesis; however, myofibroblasts, which are significant mediators of fibrosis known to produce ECM proteins, have been receiving more attention in recent years (Todd et al. 2012; Liu et al. 2017). Fibroblasts are derived from various sources, including resident fibroblasts, differentiation of bone marrow (BM)-derived cells, epithelial-to-mesenchymal transition (EMT), and endothelial-to-mesenchymal transition (EndMT) (Todd et al. 2012; Yun et al. 2020; Hasan et al. 2022). Among these, EndMT has been suggested as a critical contributor to the development of PF (Yun et al. 2020). Hashimoto et al. reported that 16.2% of fibroblasts isolated from the lung tissue of bleomycin (BLM)-induced mice were derived from local endogenous lung capillary endothelial cells (ECs), whereas the contribution of endothelial progenitor cells in the BM was minor (Hashimoto et al. 2010). In addition, lineage tracing revealed that 18% of cells isolated from the lung tissue of BLM mice showed Tie2^{+} vimentin[+] double positive cells, indicating EC-derived fibroblasts (Jia et al. 2021). These studies indicated that a significant number of fibroblasts arise from ECs via EndMT.

CONTACT Jongmin Kim ✉ jkim@sookmyung.ac.kr 📍 Division of Biological Sciences, Sookmyung Women's University, 52 Hyochangwon-gil, Yongsan-gu, Seoul, 140-742, Korea; Research Institute for Women's Health, Sookmyung Women's University, Seoul, 04310, Korea; Aram Lee ✉ aram0918@sookmyung.ac.kr 📍 Department of Life Systems, Sookmyung Women's University, 52 Hyochangwon-gil, Yongsan-gu, Seoul, 140-742, Korea

ECs play a key role in maintaining vascular homeostasis (Cho et al. 2018; Kim et al. 2019). Endothelial dysfunction caused by pathological stimuli leads to EndMT, which contributes to pathological development of diseases such as cancer, atherosclerosis, fibrosis, and pulmonary arterial hypertension (PAH) (Cho et al. 2018; Kim 2018). EndMT is a process in which ECs lose their own characteristics and gain mesenchymal characteristics (Cho et al. 2018). When EndMT occurs, ECs lose endothelial markers such as von Willebrand factor (vWF), vascular endothelial (VE)-cadherin (VE-cadherin/CDH5), and platelet and endothelial cell adhesion molecule 1 (CD31/PECAM1), and gain mesenchymal markers such as α-smooth muscle actin 2 (SMAα/ACTA2), smooth muscle protein 22 alpha (SM22α), fibroblast-specific protein 1 (FSP-1/S100A4), fibronectin, N-cadherin, and type I collagen (Cho et al. 2018; Katikireddy et al. 2018). In addition, ECs undergo morphological changes from a cobble-stone-like to a spindle-shaped fibroblast-like morphology during EndMT (Ma et al. 2020; Liu et al. 2021). Many studies have reported that EndMT occurs in the lungs of patients with IPF and IPF animal models and plays an pathological role in the development of PF (Hashimoto et al. 2010; Choi et al. 2015; Jia et al. 2021; Martin et al. 2021; Gaikwad et al. 2022). Thus, EndMT targeting strategy can be a promising therapeutic approach for the treatment of PF. However, the mechanism underlying EndMT during PF remains unclear. Therefore, further studies are required to identify therapeutic agents targeting EndMT and its molecular mechanisms.

Ginsenoside Rg3 (Rg3) is a steroidal saponin extracted from ginseng (Lee et al. 2020). Interestingly, Rg3 is known to exert vascular-protective effects. Rg3 and Rg3-enriched Korean red ginseng improved endothelial nitric oxide (NO) production and vasorelaxation, thus ameliorating blood pressure stability in spontaneously hypertensive rats (Hien et al. 2010; Park et al. 2014; Nagar et al. 2016). In addition, Rg3 protects cardiac function against adriamycin-induced injury and represses atherosclerosis by improving ox-LDL-induced endothelial dysfunction in an ApoE-/- mouse model (Wang et al. 2015; Geng et al. 2020). A recent study reported that Rg3 inhibits EMT by binding to hypoxia-inducible factor 1 alpha (HIF-1α) (Fu et al. 2021). Although the importance of EndMT in PF and the beneficial effects of Rg3 on ECs have been recognized, the effect of Rg3 on EndMT has rarely been investigated. We have previously reported that Rg3 suppresses γ-D-Glutamyl-meso-diaminopimelic acid induced EndMT (Lee et al. 2020). Based on a series of studies, we speculate that Rg3 ameliorates PF by inhibiting EndMT.

Here, we found that EndMT occurs in a BLM-induced PF mouse model, and Rg3 alleviates PF by inhibiting EndMT. Additionally, we demonstrated that Rg3 inhibited EndMT through the Smad2/3-mediated pathway. Overall, this study provides insights into the therapeutic potential of Rg3 in PF.

Materials and methods

Animals

Male C57BL/6N mice (20-25g) were purchased from Saeronbio (Gyeonggi-do, Korea) and maintained at a temperature of 20–25 °C with 12h light/dark cycle in pathogen-free environment. Total 25 mice were randomly divided into three groups: control, BLM, and BLM + Rg3 5 mg/kg groups. The mice were anesthetized and intratracheally instilled with 2 units/kg (= 1 mg/kg) body weight BLM (Sigma, Saint Louis, USA, B2434) in 50 µl of sterile phosphate buffer saline (PBS). Mice in the BLM + Rg3 group were injected intragastrically with 400 µl Rg3 (Cayman, 15332) daily for 27 days starting from the day of BLM administration. On day 28, all mice were sacrificed, and lung tissues were harvested for further experiments.

Cell culture and treatment

Human pulmonary arterial endothelial cells (HPAECs; Lonza, Basel, Switzerland) were cultured at 37 °C in a 5% CO_2 incubator with EBM-2 basal medium supplemented with EGM-2 (Lonza) and 1% penicillin-streptomycin (Welgene, Daegu, Korea). For experimental treatments, HPAECs were grown to 70–90% confluency. HPAECs were pre-treated with 10 µg/ml Rg3 (Cayman, 15332) for 24h and then incubated with 10 ng/ml transforming growth factor beta 2 (TGF-β2) (Peprotech, USA, #100-35B) and 1 ng/ml interleukin 1 beta (IL-1β) (R&D Systems, Minneapolis, USA, 201-LB-005) for designated time points.

Reagents

Rg3 was purchased from Cayman Chemical (Ann Arbor, MI, USA) and was dissolved in dimethyl sulfoxide. TGF-β2 was dissolved in distilled water containing 0.1% bovine serum albumin (BSA). IL-1β was dissolved in PBS containing 0.1% BSA. BLM was purchased from Sigma–Aldrich.

Real-time polymerase chain reaction

Total RNA was isolated using a miRNeasy RNA isolation kit (Qiagen, Hilden, Germany). For mRNA analysis,

purified RNA was reverse-transcribed using the qPCRBIO cDNA Synthesis Kit (PCR BIOSYSTEMS, London, UK). qRT-PCR was performed using the qPCRBIO SyGreen Blue Mix Lo-ROX (PCR BIOSYSTEMS) according to the manufacturer's instructions. Ribosomal 18S RNA was used as the internal control.

Western blotting

HPAECs were lysed with RIPA buffer (Gendepot, Barker, TX, USA) containing a protease and phosphatase inhibitor cocktail (Roche Diagnostics, Risch-Rotkreuz, Switzerland). Thereafter, centrifugation was performed at 13,000 rpm and 4 °C for 15 min. Protein concentrations were determined using a Pierce BCA Protein Assay (Thermo Fisher Scientific, Waltham, USA). Equal amounts of total protein were separated by sodium dodecyl sulfate–polyacrylamide gel electrophoresis and transferred onto polyvinyl difluoride membranes (Millipore, Burlington, USA). Immunoblotting was performed using primary antibodies specific to CD31 (1:2000, Cell Signaling, Danvers, USA), VE-cadherin (1:2000, Santa Cruz, Dallas, USA), Fibronectin (1:3000, Santa Cruz), N-cadherin (1:3000, BD Biosciences, Franklin Lakes, USA), SM22α (1:3000, Abcam, Cambridge, UK), vimentin (1:5000, Santa Cruz), SMAα (1:2000, Abcam), p-Smad2 (1:2000, Cell Signaling), p-Smad3 (1:2000, Cell Signaling), Smad2 (1:2000, Cell Signaling), Smad3 (1:2000, Cell Signaling), and GAPDH (1:5000, Cell Signaling). Immunodetection was accomplished using HRP-conjugated mouse (1:4000, Thermo Fisher Scientific) and rabbit (1:4000, Cell Signaling) secondary antibodies. An enhanced chemiluminescence detection method was used for development (Thermo Fisher Scientific).

Histopathological analysis

Mouse lung tissue was fixed with 10% neutral buffered formalin (NBF) for 24h, then embedded in paraffin. The paraffin blocks were sectioned at 5 μm and stained with a hematoxylin and eosin stain kit (Vector laboratories, Newark, CA, USA, H-3502) or Trichrome Stain Kit (ScyTek, TRM-2-IFU) using the manufacturer's standard procedures. Ashcroft score was used to assess fibrosis (Hubner et al. 2008). According to the scale defined by Ashcroft et al., the degree of fibrosis region in the lung was classified and analyzed from grade 0 to grade 8.

Immunofluorescence analysis

HPAECs were fixed with NBF for 5 min and washed with PBS. For permeabilization, cells were incubated with 0.1% Triton X-100 in PBS for 5 min (permeabilization was not performed for VE-cadherin staining). After blocking with 1% BSA in PBS for 1 h, the primary antibodies were applied overnight at 4 °C. VE-cadherin (1:300, Cell Signaling Technology) and SM22α (1:500, Abcam) were used. The secondary antibodies used were goat anti-rabbit Alexa Fluor 488 and 568. The sectioned mouse lung paraffin sections were deparaffinized by histoclear (Chayon, Seoul, Korea, HS-200), and antigen retrieval was performed with Borg decloaker RTU solution (Biocare Medical, Pacheco, CA, USA, BRR1000AG1) for 15 min in a high-pressure cooker. After blocking with 5% goat serum and 1% BSA in PBS for 30 min at room temperature, sections were incubated with anti-vWF-FITC (Abcam) and anti-SMAα-Cy3 (Sigma) 1:200 dilutions for overnight at 4▢. The following day, the sections were washed with PBS and mounted in VECTASHIELD HardSet Antifade Mounting Medium with DAPI (Vector Laboratories, H-1500). Immunostaining images were obtained using confocal microscopy (ZEISS LSM-700, Carl Zeiss, Oberkochen, Germany).

Dil-ac-LDL-uptake assay

HPAECs were plated in 12 well plate at a density of 2×10^5 cells/well. After drug treatments, the cells were washed twice with PBS and incubated for 30 min with 10 μg/ml 1,1′-dioctadecyl-3,3,3′,3′-tetramethylindocarbocyanine perchlorate-acetylated-low-density lipoprotein (Dil-Ac-LDL) (Invitrogen, CA, USA) in EBM2 serum-free medium. The cells were then fixed with NBF for 5 min, followed by DAPI staining for 5 min. Dil-ac-LDL uptake was observed using microscopy.

Wound healing assay

HPAECs were seeded in 12 well plate at a density of 2×10^5 cells/well and grown overnight to confluence for wound healing assay. The next day, after pre-treating Rg3 at a concentration of 10 μg/ml for 24 h, to induce EndMT, TGF-β2 and IL-1β was simultaneously treated for 24 h. The monolayer of cells was scratched using a yellow tip to create the wound. Migration closure was analyzed using Image J software.

Statistical analysis

All experiments were performed at least three times, and analyses were performed using GraphPad Prism software (version 7.0). When two groups were compared, statistical differences were assessed using an unpaired two-tailed Student's t-test. Statistical significance was determined using one-way analysis of variance followed

by Bonferroni's multiple comparison test. Statistical significance was set at $P < 0.05$.

Results

Rg3 attenuates BLM-induced PF mice

To investigate the effects of Rg3, we used a BLM-induced mouse model, which is the most common PF model (Moeller et al. 2008). We assessed the anti-fibrotic effect of Rg3 using hematoxylin and eosin (H&E) staining, Masson's trichrome staining (MTS), and Ashcroft scoring. The lung tissue of mice in the control group had a normal lung tissue structure, whereas histopathological changes, such as thicker alveolar septa, broken alveoli structure, and collagen deposition, occurred in the lung tissue of the BLM-treated group. The intraperitoneal administration of Rg3 (5 mg/kg) reversed these hallmark changes. Notably, Rg3 significantly reduced collagen deposition levels to almost those of the control group (Figure 1(a,b)). Collectively, we demonstrated that Rg3 attenuated PF in BLM-treated mice.

EndMT occurs in the lung of BLM-induced PF mice

EndMT is a key factor in vascular remodeling and has been frequently mentioned as the main source of myofibroblasts in fibrotic diseases (Pardali et al. 2017). Thus, we conducted the following experiments to identify whether EndMT appears in the lung vasculature of the BLM-induced mouse model. To examine the colocalization of EC markers and mesenchymal markers, immunofluorescence was performed on the lung tissue of mice using vWF and SMAα antibodies. We observed that the vWF⁺ SMAα⁺ double-positive area significantly increased and the smooth muscle layer thickened in the lung tissue of the BLM-treated group compared to those in the control group (Figure 2(a)). In addition, both the mRNA and protein expression of mesenchymal markers increased in the homogenized lung tissue of the BLM-treated group (Figure 2(b,c)). The number and intensity of SMAα-upregulated blood vessels of size less than 100 μm increased in the lung tissue of BLM-treated group compared to the control group (Figure 2(d)). These data indicate that EndMT occurs in the lung vasculature of BLM-induced PF mice and that EndMT may be a key contributor in the progression of PF.

Rg3 inhibits EndMT in BLM-induced PF

We have previously identified that Rg3 inhibits inflammation-induced EndMT and maintains the endothelial cell phenotype (Lee et al. 2020). In addition, based on

studies showing that Rg3 has vascular protective effects on pulmonary and cardiovascular diseases, such as lung injury, COPD, hypertension, myocardial infarction, and atherosclerosis (Hien et al. 2010; Park et al. 2014; Wang et al. 2015; Nagar et al. 2016; Zhang et al. 2016; Yang et al. 2018; Geng et al. 2020; Guan et al. 2020), we hypothesized that Rg3 alleviates BLM-induced PF through EndMT inhibition. Indeed, the colocalization percentage of vWF and SMAα significantly decreased and the smooth muscle layer was thinner in the lung tissue of the BLM/Rg3 group compared to that in the BLM-treated group (Figure 3(a)). In addition, the mRNA and protein expression levels of mesenchymal markers decreased in the homogenized lung tissue of the BLM/Rg3 group (Figure 3(b,c)). Given that we found that SMAα expression was elevated in the blood vessels of BLM-induced PF mice (Figure 2(d)), we performed immunofluorescence staining to investigate the effect of Rg3 on SMAα expression. Rg3 treatment significantly decreased the intensity of SMAα-stained region on blood vessels than BLM-treated tissue. (Figure 3(d)). Taken together, these findings indicate that Rg3 inhibits EndMT in BLM-induced PF in mice.

Rg3 inhibits EndMT induced by co-treatment with TGF-β2 and IL-1β in HPAECs

To further investigate the inhibitory effect of Rg3 on EndMT *in vitro*, EndMT was induced by co-treating HPAECs with TGF-β2 and IL-1β. Rg3 was pre-treated 24 h before co-treatment with TGF-β2 and IL-1β. We found that EndMT-induced cells lost their cobblestone-like morphology and became spindle-shape. However, ECs maintained their shape similar to that of control cells when pre-treated with Rg3 (Figure 4(a)). Rg3 treatment also significantly reversed the mRNA and protein expression levels of EC and mesenchymal markers (Figure 4(b,c)). We also analyzed the changes in the expression of these markers through immunocytochemistry and found that Rg3 treatment restored the expression of the EC marker VE-cadherin and the mesenchymal marker SM22α, which is consistent with the mRNA and protein expression results (Figure 4(d)). EndMT-induced cells not only undergo changes in morphology and marker expression, but also accompany EC dysfunction (Huang et al. 2021). Thus, we examined Ac-LDL uptake, a well-known intrinsic function of ECs (Ghosh et al. 2012), and found that the uptake ability of Dil-Ac-LDL was restored by Rg3 treatment (Figure 4(e)). Also, during the EndMT process in ECs, the cellular migratory ability gradually increases (Zhang et al. 2020). Co-treatment with TGF-β2 and IL-1β increases the migratory capacity of cells, whereas this capacity is
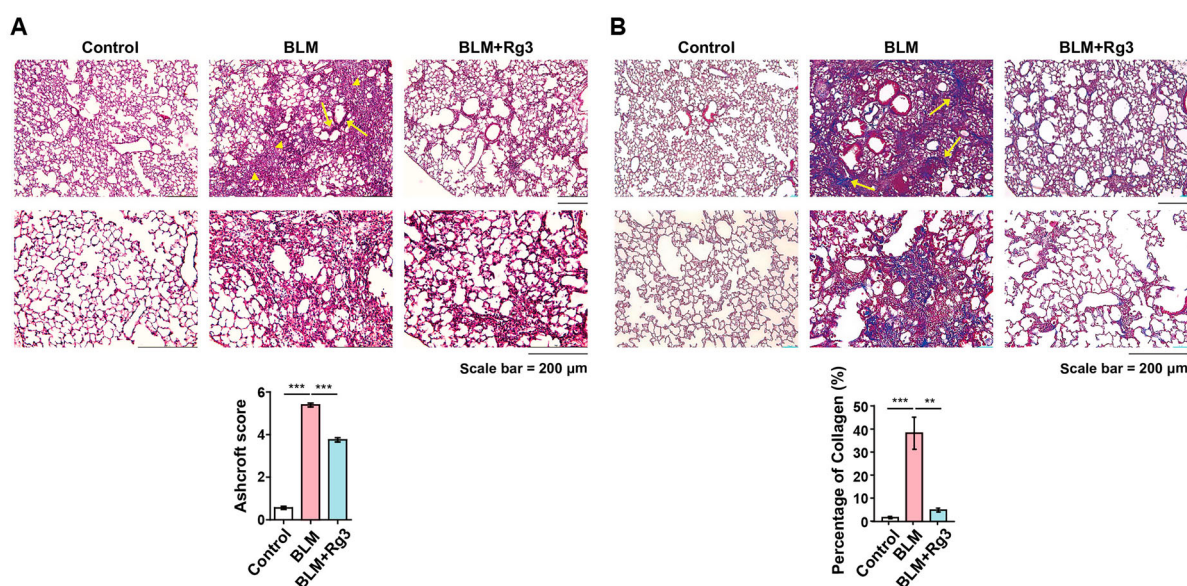
Figure 1. Rg3 mitigates BLM-induced PF. (A) H&E staining of the lung from mice injected BLM with or without Rg3. Arrows and arrowheads indicate thicker alveolar septa and broken alveoli structure, respectively. (B) Masson's trichrome staining of the lung of mice injected with or without Rg3. Arrows indicate collagen deposition. (n = 3, 4 per group) **P < 0.01, ***P < 0.001 by one-way ANOVA with Bonferroni's multiple comparison test. Error bars, s.e.m.

suppressed by Rg3 (Figure 4(f)). Taken together, these results provide insight into Rg3 as a therapeutic option for EndMT-related vascular diseases.

Rg3 inhibits EndMT by regulating Smad signaling

TGF-β signaling is a major regulator of EndMT and is associated with fibrotic diseases by activating Smad signaling and ECM deposition (Pardali et al. 2017; Cho et al. 2018; Yun et al. 2020). Therefore, we compared Smad2/3 phosphorylation in the normal, BLM, and BLM + Rg3 groups. The lung tissues of the BLM group showed significantly elevated phosphorylated Smad2/3 expression, which was decreased by Rg3 treatment (Figure 5(a)). We also examined the expression of Smad2/3 in EndMT-induced HPAECs. Since the phosphorylation of Smad increased within 30 min after exposure to TGF-β2 and IL-1β and decreased gradually until 180 min (data not shown), the following experiment was performed 30 min after exposure to TGF-β2 and IL-1β. An inhibitory effect of Rg3 on Smad2/3 phosphorylation was also observed in HPAECs (Figure 5(b)). These data suggest that Smad signaling may be a key mechanism by which Rg3 inhibits EndMT induced by co-treatment with TGF-β2 and IL-1β.

Discussion

Emerging evidence has demonstrated that EndMT contributes to various human diseases such as cancer, fibrosis, PAH, and atherosclerosis (Ma et al. 2020). It has been reported that approximately 16–18% of fibroblasts are EC-derived in PF mouse lung, 27-35% of all fibroblasts in fibrotic hearts and 30-50% of fibroblasts in fibrotic kidneys originated from ECs (Zeisberg et al. 2007; Zeisberg et al. 2008; Hashimoto et al. 2010; Jia et al. 2021). The fact that a substantial portion of fibroblasts originate from EC explains that EndMT plays a critical role in the pathogenesis of diseases. Many studies have attempted to target EndMT as a therapeutic strategy; indeed, it has been proven to be effective in fibrotic diseases, including cardiac fibrosis, diabetic kidney fibrosis, systemic sclerosis, and PAH (Zeisberg et al. 2007; Reynolds et al. 2012; Kanasaki et al. 2014; Cipriani et al. 2015; Chen et al. 2017). Several studies have demonstrated that the inhibition of EndMT has therapeutic effects in both *in vitro* and *in vivo* PF models (Choi et al. 2015; Suzuki et al. 2017; Jia et al. 2021; Pei et al. 2022). A novel HIF-1α inhibitor, 2-methoxyestradiol, suppresses irradiation-induced EndMT both *in vitro* and *in vivo* (Choi et al. 2015). Vildagliptin, a DPP-4 inhibitor, attenuated lipopolysaccharide (LPS)-induced PF in a mouse model and inhibited LPS-induced EndMT in pulmonary vascular ECs isolated from mouse lungs (Suzuki et al. 2017). A recent study reported that linagliptin, a highly specific DPP4 inhibitor, ameliorates BLM-induced EndMT both *in vitro* and *in vivo* (Pei et al. 2022). Galectin-3 antagonist also alleviated BLM-induced PF by inhibiting the AKT/GSK3β/β-catenin pathway (Jia et al. 2021).
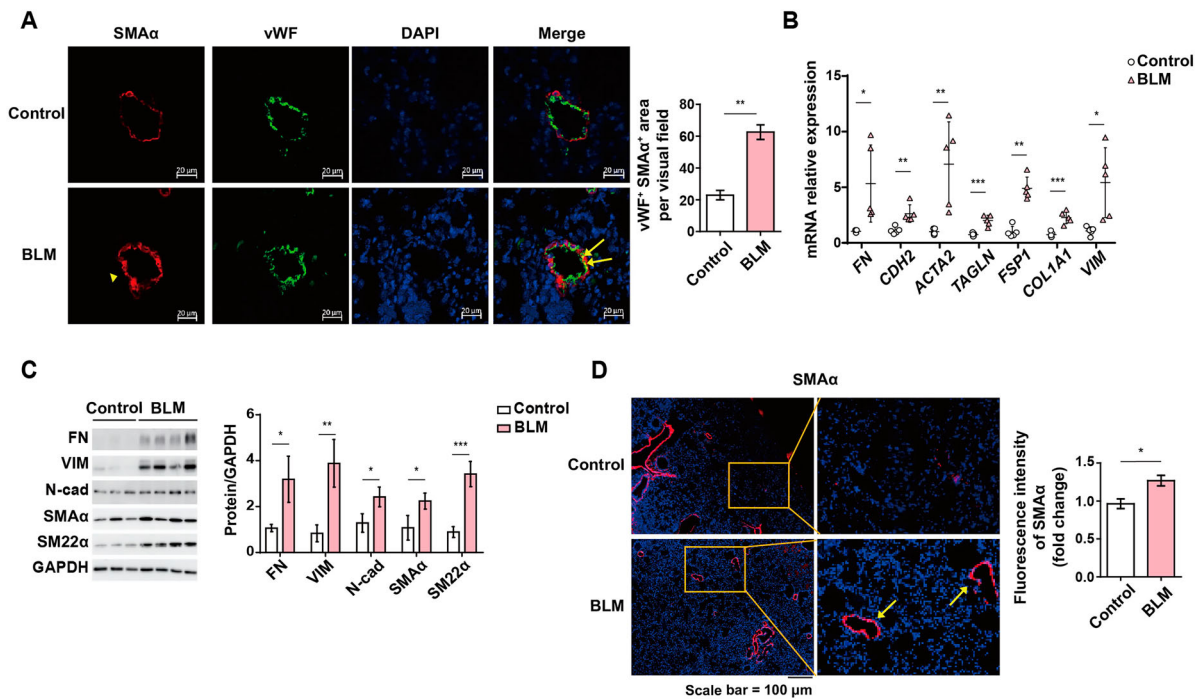
Figure 2. EndMT observed in the lung of BLM-induced PF mice. (A) Immunofluorescence staining of endothelial cell marker vWF (green), mesenchymal marker SMAα (Katikireddy et al.) and DAPI (blue) in the lung tissue of control and BLM-induced PF mice. An arrowhead indicates the thickened smooth muscle layer. Arrows indicate increased vWF$^+$ SMAα$^+$ double-positive area. The mRNA (B) and protein (C) expression of mesenchymal markers in homogenized lung tissue of BLM-treated mice. (D) Immunofluorescence staining for SMAα in the lung of control and BLM-treated mice. Arrows indicate SMAα positive blood vessels. ($n = 3$, 4 per group) *$P < 0.05$, **$P < 0.01$ compared with the controls, as determined by the unpaired two-tailed Student t test. Error bars, s.e.m.

Natural products, including plant extracts, traditional herbal medicines, and active compounds isolated from plants, are known to have positive results in the treatment of PF (Hasan et al. 2022). Ginseng is a medicinal herb, and its extract and active components exert pharmacological effects on PF (Liu et al. 2020). Ginseng extract and total saponins extracted from ginseng reduce fibrosis in the lungs of animal models of PF (Tsai et al. 2011; Liu et al. 2020; Liu et al. 2020). Among the many active components, we speculated that Rg3 could be a potent therapeutic agent based on previous studies showing that Rg3 improves endothelial function and inhibits pathological vascular remodeling (Hien et al. 2010; Geng et al. 2020; Lee et al. 2020). Although EndMT plays a critical role in the pathological events of various cardiovascular diseases, the inhibitory effect of Rg3 on EndMT has only been demonstrated in our previous study (Lee et al. 2020). Rg3 administration reduced collagen deposition and ameliorated fibrosis (Lee et al. 2020). In addition, Rg3 inhibited EndMT in the lung vasculature and decreased mesenchymal marker expression in whole lung tissue (Lee et al. 2020).

To investigate the effects of Rg3 *in vitro*, it is important to establish an *in vitro* PF model. Although TGF-β signaling is closely associated with EndMT and the pathogenesis of PF, most studies have focused on TGF-β1-induced PF (Hasan et al. 2022). However, TGF-β2 plays a key role in embryonic cardiac EndMT and is known to be a stronger EndMT inducer than TGF-β1 (Maleszewska et al. 2013). Polosukhin et al. reported that the increase in TGF-β2 expression was much more dramatic than that of TGF-β1 in the lung tissue of an early BLM-exposed mouse model (1-2 weeks) (Polosukhin et al. 2012). Additionally, IL-1β is a potent inducer of EndMT (Yun et al. 2020). Overexpression of IL-1β in rat lungs leads to progressive lung tissue fibrosis, accompanied by increased TGF-β1 expression, myofibroblast accumulation, and ECM deposition (Kolb et al. 2001). IL-1β mRNA and protein expression were elevated in the serum and lung tissues of BLM-treated mice (Cavarra et al. 2004). Several studies have demonstrated that the combination of two well-known EndMT inducers, TGF-β2 and IL-1β, leads to EndMT in various ECs including human saphenous vein ECs, human esophageal microvascular ECs, human umbilical vein ECs, and HPAECs (Maleszewska et al. 2013; Nie et al. 2014; Girao-Silva et al. 2021; Monteiro et al. 2021). Thus, we hypothesized that co-treatment with TGF-β2 and IL-1β would be a suitable *in vitro* model for mimicking EndMT in PF. Indeed, Rg3 reversed EC morphology
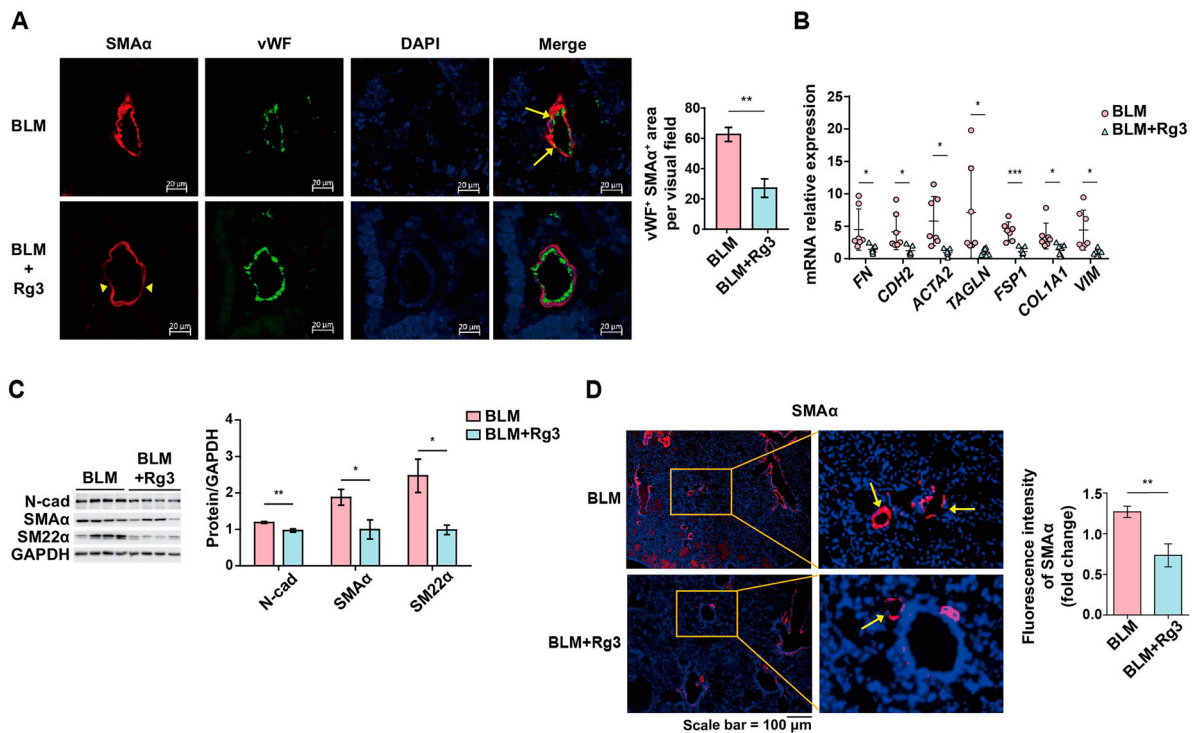
Figure 3. Rg3 restores EndMT in the lung of BLM-induced PF mice. (A) Immunofluorescence staining of EC marker (vWF) and mesenchymal marker (SMAα) in the lung tissue of BLM-induced PF mice model with or without treatment of Rg3. Arrowheads indicate thinner smooth muscle layer. The mRNA (B) and protein (C) expression of mesenchymal markers in the homogenized lung tissue. The graphs show decreased level of the mesenchymal markers in BLM/Rg3 group compared to BLM group. (D) Immunofluorescence staining for SMAα in the lung tissue. Rg3 decreased SMAα stained area compared to BLM group. Arrows indicate SMAα positive blood vessels. ($n = 4$ per group) *$P < 0.05$, **$P < 0.01$, ***$P < 0.001$ by one-way ANOVA with Bonferroni's multiple comparison test. Error bars, s.e.m.

changes, EndMT marker expression, Dil-ac-LDL uptake, and migratory capacity in co-treatment with TGF-β2 and IL-1β induced HPAECs. Further studies are needed to determine whether Rg3 can effectively inhibit EndMT-derived fibroblast-like cells but not resident vascular cells.

Next, we examined the molecular mechanism of Rg3 modulating EndMT. It has been known that TGF-β induces EndMT through canonical Smad2/3 pathway (Maleszewska et al. 2013; Yun et al. 2020). We found that Rg3 significantly reduces Smad2/3 activation induced by TGF-β2 and IL-1β. In addition, phosphorylated Smad2/3 levels in the whole lung tissue of PF mice were reduced compared to that of the control group. Recently, it was reported that Rg3 interacts with HIF-1α and inhibits its nuclear translocation, thereby attenuating the progression of BLM-induced PF (Fu et al. 2021). In this study, Rg3 was administered 35 days after BLM treatment, indicating Rg3 its therapeutic effects (Fu et al. 2021). In contrast, our group administered Rg3 from the day BLM was injected, indicating a preventive effect. Furthermore, we found that pre-treatment with Rg3 inhibited EndMT *in vitro*. These results

indicate that Rg3 could be used for both prevention and treatment. Although the pharmacological effect of Rg3 on PF has been demonstrated in both prevention and treatment models, whether Rg3 inhibits EndMT through Smad2/3 signaling in an animal model requires further investigation.

Despite many efforts to discover new drugs, only nintedanib and pirfenidone have been approved for the treatment of PF (Wang et al. 2020; Jia et al. 2021; Hasan et al. 2022). They are known to have anti-fibrotic effects, delay progression, and improve the survival rate by inhibiting fibroblast proliferation, ECM production, and myofibroblast differentiation (Wollin et al. 2015; Shah et al. 2021). However, nintedanib and pirfenidone still have limitations such as short half-life, side effects, and insufficient efficacy (Warrior et al. 2021; Ma et al. 2022). There was even a report that mortality or symptom burden did not significantly change even though progression was slowed down with nintedanib treatment (Warrior et al. 2021). Therefore, more effective treatment strategies are needed. Rg3 is a better option because it shows anti-fibrotic and vascular protective effects by inhibition of EndMT, which is a
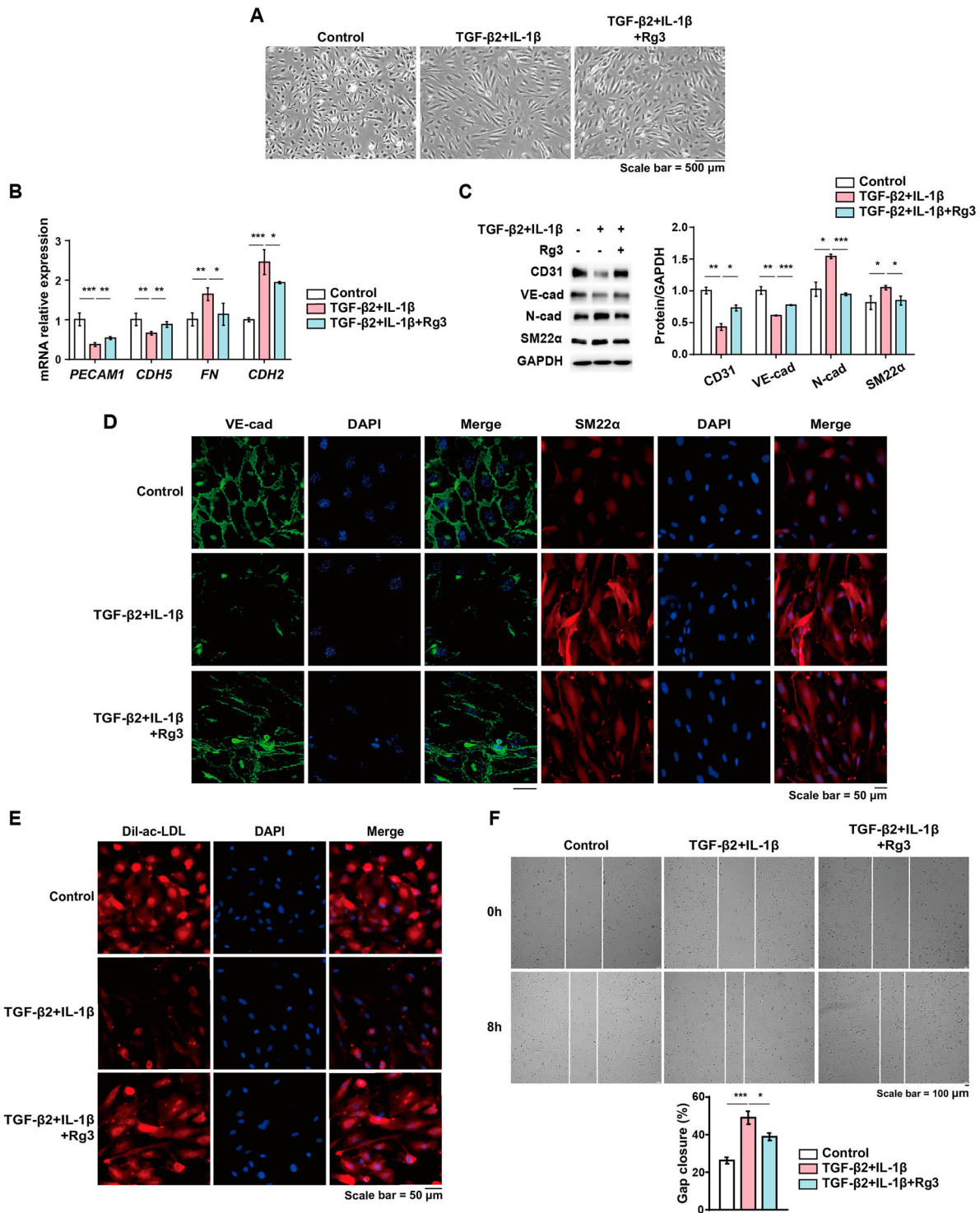
Figure 4. Rg3 ameliorates EndMT induced by co-stimulation with TGF-β2 and IL-1β in HPAECs. (A) Representative image of HPAECs in response to co-treatment with TGF-β2 (10 ng/ml) and IL-1β (1 ng/ml) with or without pretreatment with Rg3 (10 μg/ml) for 24h. The mRNA (B) and protein expressions (C) of endothelial and mesenchymal markers. The graphs show restored EC and mesenchymal marker expression by Rg3 treatment. (D) Immunofluorescence staining images of EC marker (VE-cad) and mesenchymal marker (SM22α) after co-treatment with TGF-β2 and IL-1β with or without Rg3 (10 μg/ml) in HPAECs. (E) Dil-ac-LDL uptake assay in EndMT-induced HPAECs treated with or without Rg3 (10 μg/ml). (F) Scratch wound healing assays were performed to assess ECs induced EndMT with or without Rg3 for 8 h. *$P < 0.05$, **$P < 0.01$, ***$P < 0.001$ by one-way ANOVA with Bonferroni's multiple comparison test. Error bars, s.e.m.
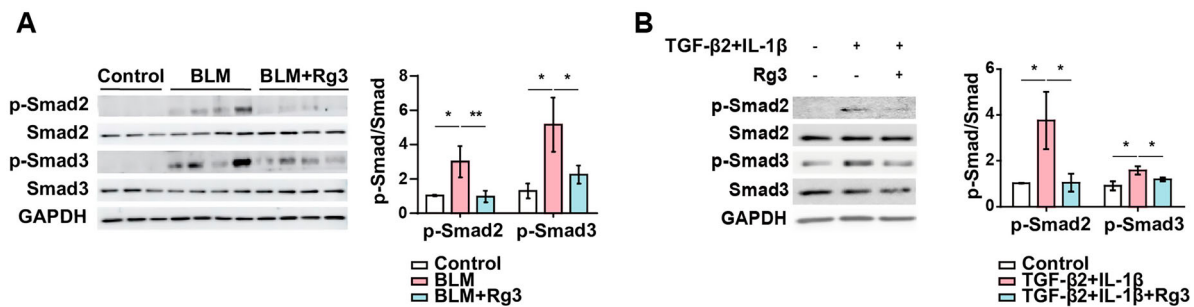
Figure 5. Rg3 suppresses EndMT through Smad signaling. (A) Protein expression of total and phosphorylated Smad2/3 in homogenized lung tissue of each group ($n = 3$, 4 per group). (B) Protein expression of total and phosphorylated Smad2/3 in whole cell lysate after exposure to TGF-β2 (10 ng/ml) and IL-1β (1 ng/ml) with or without concurrent treatment with Rg3 (10 μg/mL). *$P < 0.05$, **$P < 0.01$, ***$P < 0.001$ by one-way ANOVA with Bonferroni's multiple comparison test. Error bars, s.e.m.

feature of fibrotic disease. The main characteristic of EndMT is a reversible process, which means that Rg3 can not only prevent fibroblast formation from ECs, but also reverse fibroblast-like cells that have already undergone EndMT in the original state. Moreover, our study provides an insight that EndMT inhibition by Rg3 can be used for the treatment of other EndMT-associated diseases as well as PF. It has been reported that Rg3 inhibits tumor proliferation, metastasis, and invasion (Meng et al. 2019; Nakhjavani et al. 2021). Rg3 has been confirmed to help overcome chemotherapy resistance in lung cancer clinical trials (Lu et al. 2008; Peng et al. 2020). This may be advantageous for applications in other diseases, as a certain level of safety and effects has been demonstrated. However, as Rg3 has been reported to have controversial effects on vascular smooth muscle cells (VSMC), a thorough investigation is required for its clinical application in vascular diseases (Zhu et al. 2021).

In conclusion, we showed that EndMT occurs in the lung tissue of a BLM-induced mouse model and Rg3 attenuates PF by inhibiting EndMT. Furthermore, we demonstrated that Rg3 reversed co-treatment with TGF-β2 and IL-1β-induced EndMT by inhibiting Smad2/3 activation both *in vivo* and *in vitro*. Targeting EndMT may be a potential therapeutic strategy because fibroblasts originating from ECs are the main pathological cause of fibrotic disease. In addition, endothelial dysfunction caused by EndMT leads to the progression of PF. Thus, Rg3 is an appropriate candidate for PF treatment that maintains vascular function and homeostasis by inhibiting EndMT. We also suggest that Rg3 could be applied to various EndMT-related diseases.

CRediT author statement

Eunsik Yun: Conceptualization, Methodology, Formal analysis, Investigation, Writing – original draft,

Visualization. **Byung Su Kwon:** Conceptualization, Supervision, Project administration. **Jongmin Kim:** Conceptualization, Project administration, Supervision, Writing – review & editing, Funding acquisition. **Aram Lee:** Conceptualization, Visualization, Supervision, Writing – review & editing, Funding acquisition.

Disclosure statement

No potential conflict of interest was reported by the author(s).

Funding

References

Assayag M, Goldstein S, Samuni A, Berkman N. 2021. 3-Carbamoyl-proxyl nitroxide radicals attenuate bleomycin-induced pulmonary fibrosis in mice. Free Radic Biol Med. 171:135–142. doi:10.1016/j.freeradbiomed.2021.05.010.

Cavarra E, Carraro F, Fineschi S, Naldini A, Bartalesi B, Pucci A, Lungarella G. 2004. Early response to bleomycin is characterized by different cytokine and cytokine receptor profiles in lungs. Am J Physiol Lung Cell Mol Physiol. 287(6):L1186–1192. doi:10.1152/ajplung.00170.2004.

Chen Y, Yuan T, Zhang H, Yan Y, Wang D, Fang L, Lu Y, Du G. 2017. Activation of Nrf2 attenuates pulmonary vascular remodeling via inhibiting endothelial-to-mesenchymal transition: an insight from a plant polyphenol. Int J Biol Sci. 13 (8):1067–1081. doi:10.7150/ijbs.20316.

Cho JG, Lee A, Chang W, Lee MS, Kim J. 2018. Endothelial to mesenchymal transition represents a Key link in the interaction between inflammation and endothelial dysfunction. Front Immunol. 9:294. doi:10.3389/fimmu.2018.00294.

Choi SH, Hong ZY, Nam JK, Lee HJ, Jang J, Yoo RJ, Lee YJ, Lee CY, Kim KH, Park S, et al. 2015. A hypoxia-induced vascular

endothelial-to-mesenchymal transition in development of radiation-induced pulmonary fibrosis. Clin Cancer Res. 21 (16):3716–3726. doi:10.1158/1078-0432.CCR-14-3193.

Cipriani P, Di Benedetto P, Ruscitti P, Capece D, Zazzeroni F, Liakouli V, Pantano I, Berardicurti O, Carubbi F, Pecetti G, et al. 2015. The endothelial-mesenchymal transition in systemic sclerosis Is induced by endothelin-1 and transforming growth factor-β and may be blocked by macitentan, a dual endothelin-1 receptor antagonist. J Rheumatol. 42 (10):1808–1816. doi:10.3899/jrheum.150088.

Fu Z, Xu YS, Cai CQ. 2021. Ginsenoside Rg3 inhibits pulmonary fibrosis by preventing HIF-1α nuclear localisation. BMC Pulm Med. 21(1):70. doi:10.1186/s12890-021-01426-5.

Gaikwad AV, Lu W, Dey S, Bhattarai P, Chia C, Larby J, Haug G, Myers S, Jaffar J, Westall G, et al. 2022. Vascular remodelling in idiopathic pulmonary fibrosis patients and its detrimental effect on lung physiology: potential role of endothelial-to-mesenchymal transition. ERJ Open Res. 8(1.

Geng J, Fu W, Yu X, Lu Z, Liu Y, Sun M, Yu P, Li X, Fu L, Xu H, et al. 2020. Ginsenoside Rg3 alleviates ox-LDL induced endothelial dysfunction and prevents atherosclerosis in ApoE −/− mice by regulating PPARγ/FAK signaling pathway. Front Pharmacol. 11:500. doi:10.3389/fphar.2020.00500.

Ghosh AK, Nagpal V, Covington JW, Michaels MA, Vaughan DE. 2012. Molecular basis of cardiac endothelial-to-mesenchymal transition (EndMT): differential expression of microRNAs during EndMT. Cell Signal. 24(5):1031–1036. doi:10.1016/j.cellsig.2011.12.024.

Girao-Silva T, Fonseca-Alaniz MH, Ribeiro-Silva JC, Lee J, Patil NP, Dallan LA, Baker AB, Harmsen MC, Krieger JE, Miyakawa AA. 2021. High stretch induces endothelial dysfunction accompanied by oxidative stress and actin remodeling in human saphenous vein endothelial cells. Sci Rep. 11(1):13493. doi:10.1038/s41598-021-93081-3.

Guan X, Yuan Y, Wang G, Zheng R, Zhang J, Dong B, Ran N, Hsu AC, Wang C, Wang F. 2020. Ginsenoside Rg3 ameliorates acute exacerbation of COPD by suppressing neutrophil migration. Int Immunopharmacol. 83:106449. doi:10.1016/j.intimp.2020.106449.

Hasan M, Paul NC, Paul SK, Saikat ASM, Akter H, Mandal M, Lee SS. 2022. Natural product-based potential therapeutic interventions of pulmonary fibrosis. Molecules. 27(5):1481. doi:10.3390/molecules27051481.

Hashimoto N, Phan SH, Imaizumi K, Matsuo M, Nakashima H, Kawabe T, Shimokata K, Hasegawa Y. 2010. Endothelial-mesenchymal transition in bleomycin-induced pulmonary fibrosis. Am J Respir Cell Mol Biol. 43(2):161–172. doi:10.1165/rcmb.2009-0031OC.

Hien TT, Kim ND, Pokharel YR, Oh SJ, Lee MY, Kang KW. 2010. Ginsenoside Rg3 increases nitric oxide production via increases in phosphorylation and expression of endothelial nitric oxide synthase: essential roles of estrogen receptor-dependent PI3-kinase and AMP-activated protein kinase. Toxicol Appl Pharmacol. 246(3):171–183. doi:10.1016/j.taap.2010.05.008.

Huang Q, Gan Y, Yu Z, Wu H, Zhong Z. 2021. Endothelial to mesenchymal transition: an insight in atherosclerosis. Front Cardiovasc Med. 8:734550. doi:10.3389/fcvm.2021.734550.

Hubner RH, Gitter W, El Mokhtari NE, Mathiak M, Both M, Bolte H, Freitag-Wolf S, Bewig B. 2008. Standardized quantification of pulmonary fibrosis in histological samples. Biotechniques. 44(4):507–511. doi:10.2144/000112729.

Jia W, Wang Z, Gao C, Wu J, Wu Q. 2021. Trajectory modeling of endothelial-to-mesenchymal transition reveals galectin-3 as a mediator in pulmonary fibrosis. Cell Death Dis. 12(4):327. doi:10.1038/s41419-021-03603-0.

Kai Y, Tomoda K, Yoneyama H, Kitabatake M, Nakamura A, Ito T, Yoshikawa M, Kimura H. 2017. Silencing of carbohydrate sulfotransferase 15 hinders murine pulmonary fibrosis development. Mol Ther Nucleic Acids. 6:163–172. doi:10.1016/j.omtn.2016.12.008.

Kanasaki K, Shi S, Kanasaki M, He J, Nagai T, Nakamura Y, Ishigaki Y, Kitada M, Srivastava SP, Koya D. 2014. Linagliptin-mediated DPP-4 inhibition ameliorates kidney fibrosis in streptozotocin-induced diabetic mice by inhibiting endothelial-to-mesenchymal transition in a therapeutic regimen. Diabetes. 63(6):2120–2131. doi:10.2337/db13-1029.

Katikireddy KR, White TL, Miyajima T, Vasanth S, Raoof D, Chen Y, Price MO, Price FW, Jurkunas UV. 2018. NQO1 downregulation potentiates menadione-induced endothelial-mesenchymal transition during rosette formation in Fuchs endothelial corneal dystrophy. Free Radic Biol Med. 116:19–30. doi:10.1016/j.freeradbiomed.2017.12.036.

Kim J. 2018. MicroRNAs as critical regulators of the endothelial to mesenchymal transition in vascular biology. BMB Rep. 51 (2):65–72. doi:10.5483/BMBRep.2018.51.2.011.

Kim SM, Huh JW, Kim EY, Shin MK, Park JE, Kim SW, Lee W, Choi B, Chang EJ. 2019. Endothelial dysfunction induces atherosclerosis: increased aggrecan expression promotes apoptosis in vascular smooth muscle cells. BMB Rep. 52(2):145–150. doi:10.5483/BMBRep.2019.52.2.282.

Kolb M, Margetts PJ, Anthony DC, Pitossi F, Gauldie J. 2001. Transient expression of IL-1β induces acute lung injury and chronic repair leading to pulmonary fibrosis. J Clin Invest. 107(12):1529–1536. doi:10.1172/JCI12568.

Lee A, Yun E, Chang W, Kim J. 2020. Ginsenoside Rg3 protects against iE-DAP–induced endothelial-to-mesenchymal transition by regulating the miR-139-5p–NF-κB axis. J Ginseng Res. 44(2):300–307. doi:10.1016/j.jgr.2019.01.003.

Liu H, Lv C, Lu J. 2020a. Panax ginseng C. A. Meyer as a potential therapeutic agent for organ fibrosis disease. Chin Med. 15(1):124. doi:10.1186/s13020-020-00400-3.

Liu M, Zhang T, Zang C, Cui X, Li J, Wang G. 2020b. Preparation, optimization, and in vivo evaluation of an inhaled solution of total saponins of Panax notoginseng and its protective effect against idiopathic pulmonary fibrosis. Drug Deliv. 27 (1):1718–1728. doi:10.1080/10717544.2020.1856222.

Liu S, Xu DS, Li M, Zhang Y, Li Q, Li TT, Ren LQ. 2021. Icariin attenuates endothelial-mesenchymal transition via H19/miR-148b-3p/ELF5 in ox-LDL-stimulated HUVECs. Mol Ther Nucleic Acids. 23:464–475. doi:10.1016/j.omtn.2020.11.021.

Liu YM, Nepali K, Liou JP. 2017. Idiopathic pulmonary fibrosis: current status, recent progress, and emerging targets. J Med Chem. 60(2):527–553. doi:10.1021/acs.jmedchem.6b00935.

Lu P, Su W, Miao ZH, Niu HR, Liu J, Hua QL. 2008. Effect and mechanism of ginsenoside Rg3 on postoperative life span of patients with non-small cell lung cancer. Chin J Integr Med. 14(1):33–36. doi:10.1007/s11655-007-9002-6.

Ma H, Liu S, Li S, Xia Y. 2022. Targeting growth factor and cytokine pathways to treat idiopathic pulmonary fibrosis. Front Pharmacol. 13:918771. doi:10.3389/fphar.2022.918771.

Ma J, Sanchez-Duffhues G, Goumans MJ, Ten Dijke P. 2020. TGF-β-Induced endothelial to mesenchymal transition in

disease and tissue engineering. Front Cell Dev Biol. 8:260. doi:10.3389/fcell.2020.00260.

Maleszewska M, Moonen JR, Huijkman N, van de Sluis B, Krenning G, Harmsen MC. 2013. IL-1β and TGFβ2 synergistically induce endothelial to mesenchymal transition in an NFκB-dependent manner. Immunobiology. 218(4):443–454. doi:10.1016/j.imbio.2012.05.026.

Martin M, Zhang J, Miao Y, He M, Kang J, Huang HY, Chou CH, Huang TS, Hong HC, Su SH, et al. 2021. Role of endothelial cells in pulmonary fibrosis via SREBP2 activation. JCI Insight. 6(22). doi:10.1172/jci.insight.125635.

Meng L, Ji R, Dong X, Xu X, Xin Y, Jiang X. 2019. Antitumor activity of ginsenoside Rg3 in melanoma through downregulation of the ERK and Akt pathways. Int J Oncol. 54 (6):2069–2079.

Moeller A, Ask K, Warburton D, Gauldie J, Kolb M. 2008. The bleomycin animal model: a useful tool to investigate treatment options for idiopathic pulmonary fibrosis? Int J Biochem Cell Biol. 40(3):362–382. doi:10.1016/j.biocel.2007.08.011.

Monteiro JP, Rodor J, Caudrillier A, Scanlon JP, Spiroski AM, Dudnakova T, Pfluger-Muller B, Shmakova A, von Kriegsheim A, Deng L, et al. 2021. Mir503hg loss promotes endothelial-to-mesenchymal transition in vascular disease. Circ Res. 128(8):1173–1190. doi:10.1161/CIRCRESAHA.120.318124.

Nagar H, Choi S, Jung SB, Jeon BH, Kim CS. 2016. Rg3-enriched Korean Red Ginseng enhances blood pressure stability in spontaneously hypertensive rats. Integr Med Res. 5(3):223–229. doi:10.1016/j.imr.2016.05.006.

Nakhjavani M, Smith E, Yeo K, Palethorpe HM, Tomita Y, Price TJ, Townsend AR, Hardingham JE. 2021. Anti-Angiogenic properties of Ginsenoside Rg3 epimers: in Vitro assessment of single and combination treatments. Cancers (Basel). 13(9.

Nie L, Lyros O, Medda R, Jovanovic N, Schmidt JL, Otterson MF, Johnson CP, Behmaram B, Shaker R, Rafiee P. 2014. Endothelial-mesenchymal transition in normal human esophageal endothelial cells cocultured with esophageal adenocarcinoma cells: role of IL-1β and TGF-β2. Am J Physiol Cell Physiol. 307(9):C859–877. doi:10.1152/ajpcell.00081.2014.

Pardali E, Sanchez-Duffhues G, Gomez-Puerto MC, Ten Dijke P. 2017. TGF-beta-Induced endothelial-mesenchymal transition in fibrotic diseases. Int J Mol Sci. 18(10.

Park JB, Kwon SK, Nagar H, Jung SB, Jeon BH, Kim CS, Oh JH, Song HJ, Kim CS. 2014. Rg3-enriched Korean Red Ginseng improves vascular function in spontaneously hypertensive rats. J Ginseng Res. 38(4):244–250. doi:10.1016/j.jgr.2014.05.011.

Pei B, Zhang N, Pang T, Sun G. 2022. Linagliptin ameliorates pulmonary fibrosis in systemic sclerosis mouse model via inhibition of endothelial-to-mesenchymal transition. Mol Cell Biochem. 477(4):995–1007. doi:10.1007/s11010-021-04349-1.

Peng Z, Wu WW, Yi P. 2020. The efficacy of Ginsenoside Rg3 combined with first-line chemotherapy in the treatment of advanced Non-small cell lung cancer in China: a systematic review and meta-analysis of randomized clinical trials. Front Pharmacol. 11:630825. doi:10.3389/fphar.2020.630825.

Polosukhin VV, Degryse AL, Newcomb DC, Jones BR, Ware LB, Lee JW, Loyd JE, Blackwell TS, Lawson WE. 2012. Intratracheal bleomycin causes airway remodeling and airflow obstruction in mice. Exp Lung Res. 38:135–146. doi:10.3109/01902148.2012.658595.

Reynolds AM, Holmes MD, Danilov SM, Reynolds PN. 2012. Targeted gene delivery of BMPR2 attenuates pulmonary hypertension. Eur Respir J. 39(2):329–343. doi:10.1183/09031936.00187310.

Roh JS, Jeong H, Lee B, Song BW, Han SJ, Sohn DH, Lee SG. 2021. Mirodenafil ameliorates skin fibrosis in bleomycin-induced mouse model of systemic sclerosis. Anim Cells Syst (Seoul). 25(6):387–395. doi:10.1080/19768354.2021.1995486.

Shah PV, Balani P, Lopez AR, Nobleza CMN, Siddiqui M, Khan S. 2021. A review of pirfenidone as an anti-fibrotic in idiopathic pulmonary fibrosis and Its probable role in other diseases. Cureus. 13(1):e12482.

Suzuki T, Tada Y, Gladson S, Nishimura R, Shimomura I, Karasawa S, Tatsumi K, West J. 2017. Vildagliptin ameliorates pulmonary fibrosis in lipopolysaccharide-induced lung injury by inhibiting endothelial-to-mesenchymal transition. Respir Res. 18(1):177. doi:10.1186/s12931-017-0660-4.

Todd NW, Luzina IG, Atamas SP. 2012. Molecular and cellular mechanisms of pulmonary fibrosis. Fibrogenesis Tissue Repair. 5(1):11. doi:10.1186/1755-1536-5-11.

Tsai KD, Yang SM, Lee JC, Wong HY, Shih CM, Lin TH, Tseng MJ, Chen W. 2011. Panax notoginseng attenuates bleomycin-induced pulmonary fibrosis in mice. Evid Based Complement Alternat Med. 2011:404761.

Wang J, Li X, Zhong M, Wang Y, Zou L, Wang M, Gong X, Wang X, Zhou C, Ma X, et al. 2020. miR-301a suppression within fibroblasts limits the progression of fibrosis through the TSC1/mTOR pathway. Mol Ther Nucleic Acids. 21:217–228.

Wang X, Chen L, Wang T, Jiang X, Zhang H, Li P, Lv B, Gao X. 2015. Ginsenoside Rg3 antagonizes adriamycin-induced cardiotoxicity by improving endothelial dysfunction from oxidative stress via upregulating the Nrf2-ARE pathway through the activation of akt. Phytomedicine. 22(10):875–884. doi:10.1016/j.phymed.2015.06.010.

Warrior K, Chung PA, Reid M, Bemiss BC. 2021. Use of nintedanib and pirfenidone in non-idiopathic pulmonary fibrosis lung disease. Am J Respir Crit Care Med. 204(1):92–94. doi:10.1164/rccm.202012-4356RR.

Wollin L, Wex E, Pautsch A, Schnapp G, Hostettler KE, Stowasser S, Kolb M. 2015. Mode of action of nintedanib in the treatment of idiopathic pulmonary fibrosis. Eur Respir J. 45 (5):1434–1445. doi:10.1183/09031936.00174914.

Yang J, Li S, Wang L, Du F, Zhou X, Song Q, Zhao J, Fang R. 2018. Ginsenoside Rg3 attenuates lipopolysaccharide-induced acute lung injury via MerTK-dependent activation of the PI3K/AKT/mTOR pathway. Front Pharmacol. 9:850. doi:10.3389/fphar.2018.00850.

Yun E, Kook Y, Yoo KH, Kim KI, Lee MS, Kim J, Lee A. 2020. Endothelial to mesenchymal transition in pulmonary vascular diseases. Biomedicines. 8(12.

Zeisberg EM, Potenta SE, Sugimoto H, Zeisberg M, Kalluri R. 2008. Fibroblasts in kidney fibrosis emerge via endothelial-to-mesenchymal transition. J Am Soc Nephrol. 19 (12):2282–2287. doi:10.1681/ASN.2008050513.

Zeisberg EM, Tarnavski O, Zeisberg M, Dorfman AL, McMullen JR, Gustafsson E, Chandraker A, Yuan X, Pu WT, Roberts AB, et al. 2007. Endothelial-to-mesenchymal transition contributes to cardiac fibrosis. Nat Med. 13(8):952–961. doi:10.1038/nm1613.

Zhang LP, Jiang YC, Yu XF, Xu HL, Li M, Zhao XZ, Sui DY. 2016. Ginsenoside Rg3 improves cardiac function after myocardial ischemia/reperfusion via attenuating apoptosis and inflammation. Evid Based Complement Alternat Med. 2016:6967853.

Zhang Y, Li C, Huang Y, Zhao S, Xu Y, Chen Y, Jiang F, Tao L, Shen X. 2020. A risk score system based on DNA methylation levels and a nomogram survival model for lung squamous cell carcinoma. Int J Mol Med. 46(1):252–264. doi:10.3892/ijmm.2020.4590.

Zhu GX, Zuo JL, Xu L, Li SQ. 2021. Ginsenosides in vascular remodeling: cellular and molecular mechanisms of their therapeutic action. Pharmacol Res. 169:105647. doi:10.1016/j.phrs.2021.105647